THE JOURNAL OF BIOLOGICAL CHEMISTRY VOL. 289, NO. 27, pp. 18668–18679, July 4, 2014

A Novel Regulatory Locus of Phosphorylation in the C Terminus of the Potassium Chloride Cotransporter KCC2 That Interferes with *N*-Ethylmaleimide or Staurosporine-mediated Activation*◆

Received for publication, March 25, 2014, and in revised form, May 15, 2014 Published, JBC Papers in Press, May 21, 2014, DOI 10.1074/jbc.M114.567834

Maren Weber‡, Anna-Maria Hartmann‡§, Timo Beyer‡, Anne Ripperger‡, and Hans Gerd Nothwang‡¶1

From the ‡Neurogenetics Group, Center of Excellence Hearing4All, School of Medicine and Health Sciences, §Systematics and Evolutionary Biology Group, Institute for Biology and Environmental Sciences, and the ¶Research Center for Neurosensory Sciences, Carl von Ossietzky University Oldenburg, 26111 Oldenburg, Germany

Background: KCC2 is a potassium-chloride cotransporter essential for hyperpolarizing neurotransmission and is associated with multiple neurological disorders.
Results: Thr^{934} and Ser^{937} are major regulatory sites of KCC2 activity, and their status influences other activation processes.
Conclusion: Thr^{934} and Ser^{937} phosphorylation increases KCC2 transport kinetics.
Significance: This study identifies a novel C-terminal KCC2 stimulatory phosphorylation site.

The neuron-specific cation chloride cotransporter KCC2 plays a crucial role in hyperpolarizing synaptic inhibition. Transporter dysfunction is associated with various neurological disorders, raising interest in regulatory mechanisms. Phosphorylation has been identified as a key regulatory process. Here, we retrieved experimentally observed phosphorylation sites of KCC2 from public databases and report on the systematic analysis of six phosphorylated serines, Ser^{25}, Ser^{26}, Ser^{937}, Ser^{1022}, Ser^{1025}, and Ser^{1026}. Alanine or aspartate substitutions of these residues were analyzed in HEK-293 cells. All mutants were expressed in a pattern similar to wild-type KCC2 ($KCC2^{WT}$). Tl^+ flux measurements demonstrated unchanged transport activity for Ser^{25}, Ser^{26}, Ser^{1022}, Ser^{1025}, and Ser^{1026} mutants. In contrast, $KCC2^{S937D}$, mimicking phosphorylation, resulted in a significant up-regulation of transport activity. Aspartate substitution of Thr^{934}, a neighboring putative phosphorylation site, resulted in a comparable increase in KCC2 transport activity. Both $KCC2^{T934D}$ and $KCC2^{S937D}$ mutants were inhibited by the kinase inhibitor staurosporine and by *N*-ethylmaleimide, whereas $KCC2^{WT}$, $KCC2^{T934A}$, and $KCC2^{S937A}$ were activated. The inverse staurosporine effect on aspartate *versus* alanine substitutions reveals a cross-talk between different phosphorylation sites of KCC2. Immunoblot and cell surface labeling experiments detected no alterations in total abundance or surface expression of $KCC2^{T934D}$ and $KCC2^{S937D}$ compared with $KCC2^{WT}$. These data reveal kinetic regulation of transport activity by these residues. In summary, our data identify a novel key regulatory phosphorylation site of KCC2 and a functional interaction between different conformation-changing post-translational modifications. The action of pharmacological agents aimed to modulate KCC2 activity for therapeutic benefit might therefore be highly context-specific.

The K^+-Cl^- cotransporter (KCC)[2] 2 is a neuron-specific secondary-active plasma membrane protein (1). In the mature brain, KCC2 is a very effective outward-directed K^+ and Cl^- cotransporter (2, 3). Its activity generates a Cl^- reversal potential more negative than the resting membrane potential (4, 5). As a consequence, the opening of ligand-gated ionotropic GABA and glycine receptors leads to a Cl^- influx mediating hyperpolarization of the neuron (3, 6, 7). Therefore, the protein is essential for fast synaptic inhibition. Mice with disruption of the gene *Slc12a5* encoding KCC2 die shortly after birth due to motor deficits, including respiratory failure (7). In addition to its transport activity, transport-independent roles in synaptogenesis, neuronal differentiation, and migration have been identified, making KCC2 a multifunctional protein (8, 9).

Sequence similarities and functional properties have assigned KCC2 to the *Slc12* family of cation chloride cotransporters. In mammals, the family consists of the inward transporters NCC, NKCC1, and NKCC2, the chloride outward transporters KCC1–4, and the chloride transporter-interacting protein CIP1 (10–12). Furthermore, the orphan transporter CCC9[3] might be part of this group (10). Paralog KCCs share a sequence identity of >67%, with KCC1 and KCC3 and with KCC2 and KCC4 forming sister groups (12, 13). Paralog NKCC and NCCs share a sequence identity of >50% (12, 13). Phylogenetic analyses revealed the presence of KCC2 in all vertebrates (10, 11), and KCC-like proteins also occur across Eukaryota (10, 11).

Dysregulation of KCC2 is associated with various human neurological disorders (11, 14), such as epileptic activity (15–

* This work was supported by Deutsche Forschungsgemeinschaft Grants No428/3-1 and No428/4-2 (to H. G. N.) and Ha6338/2-1 (to A.-M. H).
◆ This article was selected as a Paper of the Week.
[1] To whom correspondence should be addressed: Dept. of Neurogenetics, Carl von Ossietzky University Oldenburg, 26111 Oldenburg, Germany. Tel.: 49-441-798-3932; Fax: 49-441-798-5649; E-mail: hans.g.nothwang@uni-oldenburg.de.

[2] The abbreviations used are: KCC, K-Cl cotransporter; NCC, Na-Cl cotransporter; NKCC, Na-K-Cl cotransporter; NEM; *N*-ethylmaleimide; HA, human influenza hemagglutinin.
[3] CCCP9 is a cation chloride cotransporter-interacting protein 1.

17), neuropathic pain (18, 19), spasticity (20), ischemic insults (21), and brain trauma (22).

These severe consequences of altered KCC2 function raised interest in mechanisms regulating its activity (5). On the cellular level, location in membrane rafts was shown to modify KCC2 transport activity (23, 24). On the molecular level, interaction partners such as the ATPase subunit α2 (25), CIP1 (26), Neto2 (27), and several protein kinases, including brain-specific creatine kinase (28), SPAK (29), OSR1 (30), and WNKs (31) were identified. The regulatory role of phosphorylation is in line with previous pharmacological studies. The kinase inhibitors lavendustin A, genistein (32), or staurosporine (33) altered KCC2 transport activity in cultured hippocampal neurons, and calyculin (34) and okadaic acid (35), two potent phosphatase inhibitors, blocked activation of KCCs by cell swelling. The important role of phosphorylation was corroborated by the regulatory role of several identified phosphorylation sites in KCC2 (36). Phosphorylation of human threonines Thr^{906} and Thr^{1007} reduced the intrinsic transport activity of KCC2 (37, 38). In contrast, phosphorylated Ser^{940} increased surface expression and KCC2 transport function (39) as well as membrane clustering (40). Finally, the phosphorylation status of Tyr^{903} and Tyr^{1087} also regulates KCC2 activity, although the functional consequences of phosphorylation appear to be context-dependent and require further investigation (5, 23, 36, 41, 42).

Here, we wished to further examine the role of phosphorylation for KCC2 activity. Mining of large scale phospho-proteomics data revealed several phosphorylated serines not yet analyzed. To characterize their importance, these amino acids were systematically substituted by either alanine or aspartate in the rat KCC2b isoform to mimic the dephosphorylated state (alanine) or the phosphorylated state (aspartate), respectively. Expression and transport activity of the mutants were then determined in HEK-293 cells. This approach identified Ser^{937} and the neighboring Thr^{934} as major novel regulatory phosphorylation sites for KCC2 transport activity.

MATERIALS AND METHODS

Bioinformatic Analyses—To identify native KCC2 phosphorylation from proteomics approaches, the two databases PhosphoSitePlus (43) and PHOSIDA (44) were screened using the term KCC2 as entry. Both databases contain curated data of experimentally observed post-translational modifications, primarily of human and mouse proteins, which were obtained by high resolution mass spectrometric analyses.

KCC protein sequences for a diverse selection of organisms were obtained from a combination of BLAST searches against GenBank™ and data mining of the Ensembl database and the Joint Genome Institute (www.jgi.doe.gov). We used the protein sequences of human KCC1 (NP_005063.1), KCC2 (NP_065759.1), KCC3 (NP_598408.1), and KCC4 (NP_006589.2) as query. For each protein in each target species, we saved all sequences with an E-value of at least 10^{-2}. These sequences were then reverse-blasted (BLASTp or translated BLAST) against the *Homo sapiens* protein database, and only those protein sequences were retained that showed the same CCC protein sequence of *H. sapiens* that was used as a query sequence as the best hit (E-value of at least 10^{-2}). Each obtained sequence was then aligned at the amino acid level using the default settings in MUSCLE (45), as implemented in SeaView version 4.4.2 (46) and manually improved by eye thereafter.

TABLE 1
Forward primer for site-directed mutagenesis

The abbreviations used are as follows: for, forward; mm, *Mus musculus*; other primers are designed for KCC2 from *Rattus norvegicus*.

Phosphosite	Sequence 5′ to 3′
S25Afor	CGGCAATCCCAAGGAGGCCAGCCCCTTCATCAAC
S25Dfor	CGGCAATCCCAAGGAGGACAGCCCCTTCATCAAC
S26Afor	CAATCCCAAGGAGAGCGCCCCCTTCATCAACAGC
S26Dfor	GCAATCCCAAGGAGAGCGACCCCTTCATCAACAGCA
S25A/S26Afor	GACGGCAATCCCAAGGAGGCCGCCCCCTTCATCAACAGCAC
S25D/S26Dfor	TGACGGCAATCCCAAGGAGGACGACCCCTTCATCAACAGCACG
T906Afor	GCATACACCTACGAGAAGGCATTGGTAATGGAACAAC
T1007Afor	CAGAGAAGGTGCATCTCGCCTGGACCAAGGATAAG
T934Afor	GGAGATCCAGAGCATCGCAGATGAATCTCGGGG
T934Dfor	CGGGAGATCCAGAGCATCGATGATGAATCTCGGGGCTCC
S937Afor	TCCAGAGCATCACAGATGAAGCTCGGGGCTCC
S937Dfor	GGAGATCCAGAGCATCACAGATGAAGATCGGGGCTCCATT
T934A/S937Afor	GGAGATCCAGAGCATCGCAGATGAAGCTCGGGGCTCC
S1022Afor	AGAACAAAGGCCCCGCTCCCGTCTCCTCGG
S1022Dfor	GAAGAACAAAGGCCCCGATCCCGTCTCCTCGGAG
S1025Afor	CCAGTCCCGTCGCCTCGGAGGGG
S1025Dfor	CCCCAGTCCCGTCGACTCGGAGGGGATC
S1026Afor	CAGTCCCGTCTCCGCGGAGGGGATCAA
S1026Dfor	CCCCAGTCCCGTCTCCGATGAGGGGATCAAGGACT
*mm*T934Dfor	CGGGAGATCCAGAGCATCGATGACGAGTCTCGGGGCTCC
*mm*S937Dfor	GGAGATCCAGAGCATCACAGATGAAGATCGGGGCTCCATT

Construction of Expression Clones—Wild-type rat KCC2b (GenBank™ accession number NM_134363) and HA-tagged mouse KCC2b (GenBank™ accession number NM_020333) expression clones with an HA tag at the N terminus or in the second extracellular loop were reported previously (47, 48). Site-directed mutagenesis of KCC2b cDNA was performed according to the QuikChange mutagenesis system (Stratagene, Heidelberg, Germany). Forward oligonucleotides for the generation of the mutations are given in Table 1. All generated clones were confirmed by sequencing.

Determination of K^+-Cl^- Cotransport—Transport activity was determined by measuring Cl^--dependent uptake of Tl^+ in HEK-293 cells. Uptake measurements were done as described previously (49, 50, 47). Cells were transiently transfected with the respective construct, using TurboFect (Fermentas, Schwerte, Germany), according to the protocol provided. Briefly, 150 μl of Opti-MEM (Invitrogen), 6 μl of TurboFect (Fermentas, Karlsruhe, Germany), and ~3 μg of DNA were mixed and incubated for 20 min at room temperature prior to transfection. 24 h after transfection, HEK-293 cells were plated in a black-walled 96-well culture dish (Greiner Bio-One, Frickenhausen, Germany) at a concentration of 100,000 cells/well. The remainder of the cells were plated on a glass coverslip. After ~18 h, coverslips were processed for immunocytochemical analysis to determine transfection rates, which were routinely between 20 and 30% (Fig. 2). Cell cultures with lower transfection rates were omitted from subsequent flux measurements. The HEK-293 cells in 96-well culture dishes were processed for flux measurements by replacing the medium with 80 μl of preincubation buffer (100 mM *N*-methyl-D-glucamine, 5 mM KCl, 2 mM $CaCl_2$, 0.8 mM $MgSO_4$, 5 mM glucose, 5 mM HEPES, pH 7.4) with or without 2 μM FlouZin-2 AM dye (Invitrogen) plus 0.2% (w/v) Pluronic F-127 (Invitrogen). After incubation for 48 min at room temperature, cells were washed three times with 80 μl

of preincubation buffer and incubated for 15 min with 80 μl of preincubation buffer plus 0.1 mM ouabain to block Na^+/K^+ ATPases. Thereafter, the culture dish was inserted into a fluorometer (Fluoroskan Accent, Thermo Scientific, Bremen, Germany), and the wells were injected with 40 μl of 5× thallium stimulation buffer (12 mM Tl_2SO_4, 100 mM *N*-methyl-D-glucamine, 5 mM HEPES, 2 mM $CaSO_4$, 0.8 mM $MgSO_4$, 5 mM glucose, pH 7.4). The fluorescence across the entire cell population in a single well was measured in a kinetic dependent manner (excitation 485 nm, emission 538 nm, 1 frame in 5 s in a 200-s time span). The activity was calculated with the initial values of the slope of Tl^+-stimulated fluorescence increase by using linear regression. At least two independent DNA preparations were used per construct, giving similar results.

The effect of the thiol-alkylating reagent *N*-ethylmaleimide (NEM) or the kinase inhibitor staurosporine was determined by adding either 1 mM NEM or 8 μM staurosporine to the preincubation buffer 15 min prior to flux measurements on the cells. For statistical analysis, data groups were compared using a Student's *t* test, and $p < 0.05$ was considered as statistically significant.

Immunocytochemistry—For immunocytochemistry, HEK-293 cells were seeded on 0.1 mg/ml poly-L-lysine-coated coverslips and incubated for 36 h. After fixation for 10 min with 4% paraformaldehyde in 0.2 M phosphate buffer and three washes in PBS, cells were incubated with blocking solution (0.3% Triton X-100, 3% bovine serum albumin, 10% goat serum in PBS) for 30 min. All steps were performed at room temperature. Primary antibody solution (anti-cKCC2, directed against the C-terminal part of KCC2, 1:1,000) (51) was added in blocking solution for 30 min. After three wash steps with PBS for 5 min, the secondary antibody was added, which was conjugated to a fluorescent probe (1:1,000; Alexa Fluor 488 goat anti-rabbit (Invitrogen)). After washing, cells were mounted onto glass slides with Vectashield Hard Set (Vector Laboratories, Burlingame, CA). Photomicrographs were taken using a Laser scanning microscope (Leica TCS SP2).

Cell Surface Labeling of KCC2-HA N-term Constructs—To determine the cell surface expression of mouse $KCC2^{WT\text{-}HA\ 2nd\ loop}$, $KCC2^{T934D\text{-}HA}$, or $KCC2^{S937D\text{-}HA}$, these constructs were expressed in HEK-293 cells. After 36 h, cells were kept at 4 °C for 15 min and washed with a chilled washing solution containing 150 mM NaCl, 2.5 mM KCl, 2 mM $CaCl_2$, 2 mM $MgCl_2$, 2.5 mM HEPES, and 2 g glucose/liter. Primary antibody (mouse anti-HA, 1:250 (Covance, Heidelberg, Germany)) was added for 25 min at 4 °C, and cells were washed three times. The secondary antibody (Alexa Fluor 488 goat anti-mouse, 1:250 (Invitrogen)) was diluted in preheated (37 °C) washing solution, and cells were incubated for 10 min at 37 °C. After washing with preheated solution, cells were fixed with 4% paraformaldehyde. Fixed cells were stained as described above with anti-cKCC2 and an Alexa Fluor 594 goat anti-rabbit to detect all KCC2 protein.

For image analysis, 2048 square pixels containing 8-bit xyz-confocal pictures were taken using a Leica TCS SP5 device with an adjustable 20-fold immersion objective (oil $n = 1.514$) and a pulsed white light laser with wavelengths adjusted to 498 nm (for Alexa Fluor 488, 10% power) and 590 nm (for Alexa Fluor 594, 4% power). The following settings were applied to all images: 100% detection of fluorescence emission with linear working HyD detectors from 507 to 548 nm (for Alexa Fluor 488) and from 610 to 646 nm (for Alexa Fluor 594) with gating restriction at 498 nm (0.30 and 6.50 ns) and 590 nm (0.30 and 6.50 ns) (Leica-microsystems.com); a pinhole of 300 μm (recorded specimen thickness = 13.3 μm); and 2-fold line and frame averages. Ten to 21 images of each experiment were evaluated for mean intensity per pixel with pre-arranged FIJI software. Three to five biological replica were performed for each construct.

TABLE 2
Phosphorylation sites in PhosphoSitePlus and PHOSIDA

PhosphoSitePlus hsKCC2	PhosphoSitePlus mmKCC2	PhosphoSitePlus rnKCC2	PHOSIDA mmKCC2
Ser^{25}	Ser^{25}	Ser^{25}	Ser^{25}
Ser^{26}	Ser^{26}	Ser^{26}	Ser^{26}
Thr^{34}	Thr^{34}	Thr^{34}	Thr^{34}
Thr^{906}	Thr^{906}	Thr^{906}	Thr^{906} (Thr^{934})
Ser^{937}	Ser^{937}	Ser^{937}	Ser^{937}
Ser^{940}	Ser^{940}	Ser^{940}	Ser^{940}
Thr^{1007}	Thr^{1006}	Thr^{1007}	Thr^{1006}
Thr^{1009}	Thr^{1008}	Thr^{1009}	Thr^{1008}
Ser^{1022}	Ser^{1021}	Ser^{1022}	Ser^{1021}
Ser^{1025}	Ser^{1024}	Ser^{1025}	(Ser^{1024})
Ser^{1026}	Ser^{1025}	Ser^{1026}	Ser^{1025}

The abbreviations used are as follows: hs, *H. sapiens*; mm, *M. musculus;* rn, *R. norvegicus.*

Immunoblot Analyses—To quantify the expression of KCC2 mutants, cells were lysed in a buffer containing 150 mM NaCl, 15 mM Tris, 1% dodecyl β-D-maltoside, and 0.4% iodoacetamide. After incubation for 5 min at 25 °C, samples were centrifuged for 5 min at 125,000 × *g*. Protein amount of the supernatant was determined using the Bradford assay. 10 μg of each sample were loaded onto a 10% SDS-polyacrylamide gel system. After separation and electrotransfer onto PVDF membranes, membranes were incubated with anti-cKCC2 (dilution 1:2,000). After incubation for 2 h at room temperature, membranes were washed four times with TBS-T (20 mM Tris, 150 mM NaCl, 1% Tween, pH 7.5), and the secondary antibody donkey anti-rabbit IgG-HRP (Santa Cruz Biotechnology, Heidelberg, Germany) was applied for 1 h. After washing, bound antibodies were detected using an enhanced chemiluminescence assay (GE Healthcare) and a LAS-3000 documentation system (Fujifilm, Düsseldorf, Germany). Quantification of bands within the linear range of exposure was performed using the MultiGauge software version 3.1 (Fujifilm). Three biological replicas were performed for each construct. Data are given as means ± S.E. Significant differences between the groups were analyzed by a Student's *t* test.

RESULTS

Database Mining and Phylogenetic Pattern of KCC2 Phosphorylation Sites—To identify *bona fide* phosphorylation sites in KCC2, the databases PhosphoSitePlus and PHOSIDA were searched for KCC2 entries. These databases contain experimentally observed phosphorylation sites identified largely by mass spectrometry-based proteomic studies (43, 44). In addition to the known phosphorylation sites Thr^{906}, Ser^{940}, and Thr^{1007}, Ser^{25}, Ser^{26}, Ser^{937}, Ser^{1022}, Ser^{1025}, Ser^{1026}, Thr^{34}, and Thr^{1009} were reported to be phosphorylated in KCC2 in both

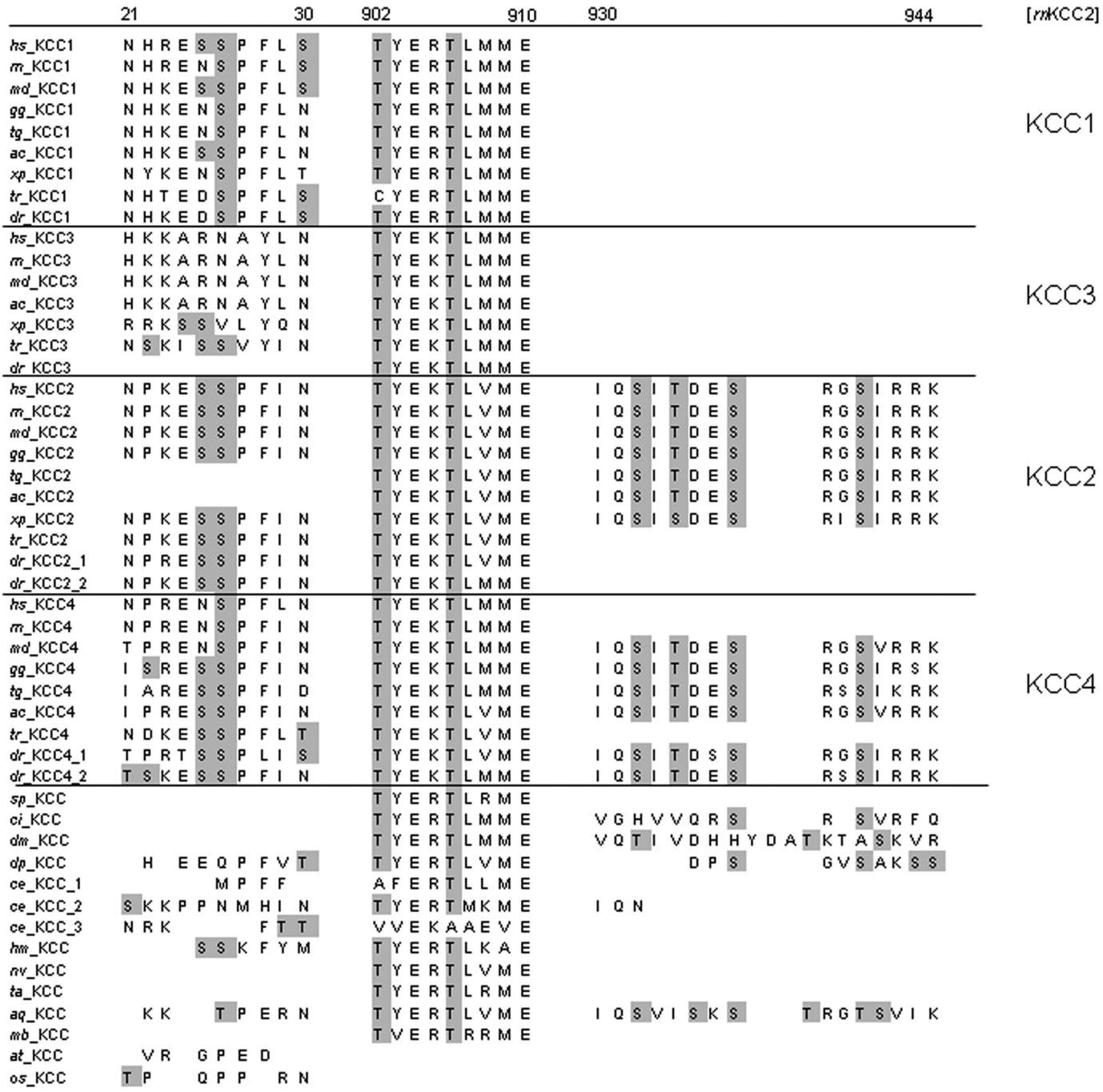

FIGURE 1. **Evolutionary conservation of phosphorylation sites and their neighboring amino acids in KCC subgroups.** Ser[25] and Ser[26] are present in most vertebrates and KCC1, KCC2, and KCC4 family members. The amino acids Thr[906] and Thr[1007] are highly conserved throughout the animal kingdom, whereas Ser[1022], Ser[1025], and Ser[1026] are highly specific to tetrapod KCC2. Ser[937], Thr[934], and Ser[940] display similar phylogenetic conservation. They are only present in vertebrate KCC2 and in non-therian KCC4. In addition to the phosphorylation sites, the five amino acids flanking either side of the corresponding phosphorylated amino acid residue are shown. Their pattern of conservation closely matched that of the respective phosphorylated amino acid residue. The abbreviations used are as follows: *mm*, *M. musculus*; *hs*, *Homo sapiens*; *rn*, *Rattus norvegicus*; *md*, *Monodelphis domestica*; *gg*, *Gallus gallus*; *tg*, *Taeniopyga gutta*; *ac*, *Anolis carolinensis*; *xt*, *Xenopus tropicalis*; *tr*, *Takifugu rubripes*; *Dr*, *Danio rerio*.

databases (numbering according to the rat KCC2b protein) (Table 2). Three of the amino acids, Ser[25], Ser[26], and Thr[34], reside in the cytoplasmic N terminus, and the remainder are located in the C-terminal part (1). Here, we focused on the six phosphoserines Ser[25], Ser[26], Ser[937], Ser[1022], Ser[1025], and Ser[1026]. Phylogenetic analyses of the KCC subfamily revealed that they cover different patterns of phylogenetic conservation. Ser[1022], Ser[1025], and Ser[1026] are highly specific to tetrapod KCC2 (Fig. 1). Ser[937] is present only in vertebrate KCC2 and in non-therian KCC4. Finally, Ser[25] and Ser[26] showed the broadest occurrence with a presence in the most vertebrate KCC1, KCC2, and KCC4 family members (Fig. 1). Notably, the previously reported amino acids Thr[906] and Thr[1007], which had been implicated in developmental activation of KCC2 during brain maturation (37), are highly conserved throughout metazoans (Fig. 1). This suggests that their phosphorylation does not only

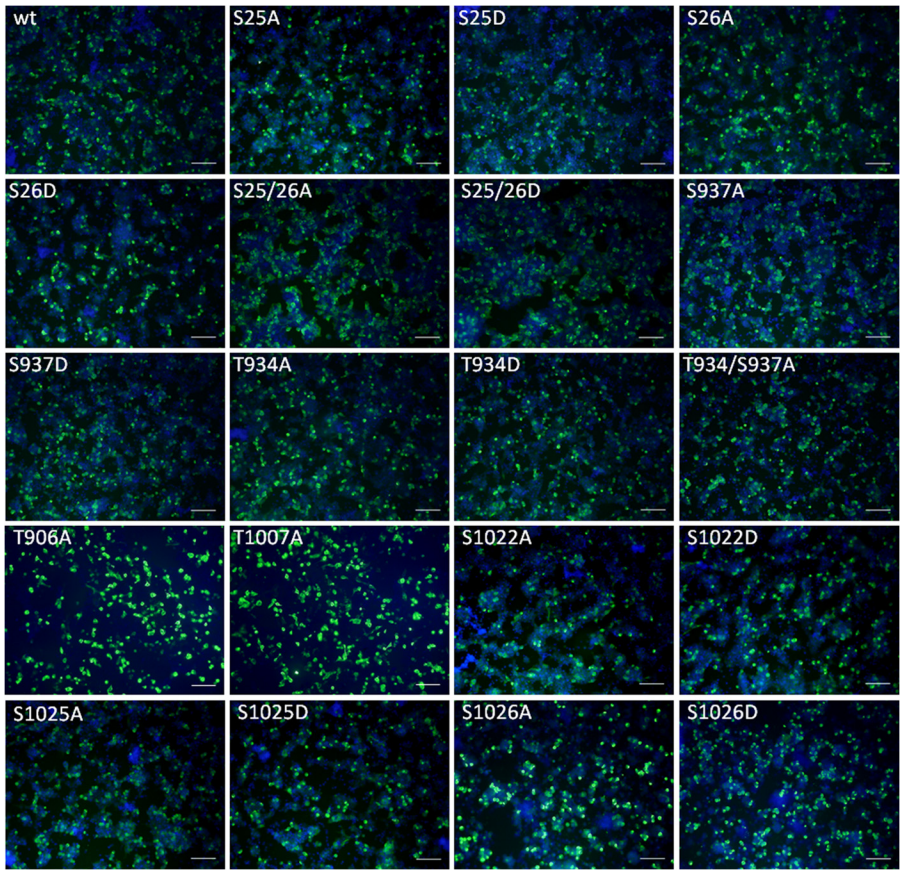

FIGURE 2. **Transfection rates of KCC2 expression constructs.** $KCC2^{WT}$ and the indicated KCC2 mutants were expressed in HEK-293 cells. To monitor transfection rates, immunocytochemistry was performed against the transporter (*green*). In parallel, cell cultures were stained with DAPI (*blue*). Typically, transfection rates between 20 and 30% were obtained. *Scale bar,* 100 μm.

play a role in vertebrate KCCs but also in those transporters from more ancient species like the choanoflagellate *Monosiga brevicolis*, which forms a sister group to the metazoan (52). Analysis of the neighboring amino acid sequences demonstrated conservation patterns very similar to those observed for the phosphorylated amino acid residues (Fig. 1). This indicates that the respective phosphorylation can also occur in other species.

Expression Analyses of KCC2 Phospho-mutants—To study the role of the phosphorylated serines Ser^{25}, Ser^{26}, Ser^{937}, Ser^{1022}, Ser^{1025}, and Ser^{1026}, we generated two mutants of rat KCC2b for each phosphorylation site. This isoform was chosen because it is the major KCC2 protein in the mature brain (53). In the following, we will refer to it as KCC2. Amino acid residues were mutated to either aspartate or alanine to mimic phosphorylated or dephosphorylated states of the respective serine. In addition, T906A and T1007A (corresponding to mouse and human Thr^{906} and Thr^{1006}) mutants were generated. They were previously shown to result in increased KCC2 activity and served as positive controls (37, 38). This resulted in 14 mutants. To check whether these mutations effect KCC2 expression, all constructs were transfected into HEK-293 cells. This cell line is most widely used to study KCC2 transport activity in a mammalian heterologous expression system (2, 37, 39, 47, 54). Immunocytochemical analyses revealed expression of all 14 mutants (Figs. 2 and 3). Immunoreactivity was detected for all mutants both at the plasma membrane and inside the cells (Fig. 3). Only the nucleus was spared. Compared with wild-type KCC2 ($KCC2^{WT}$), no difference in subcellular localization was obvious upon visual inspection. Thus, all mutants were well expressed in HEK-293 cells.

Transport Activity of KCC2 Phospho-mutants—In a first series of experiments, we focused on the two N-terminal Ser^{25} and Ser^{26} phosphorylation sites and determined their activity in HEK-293 cells using Tl^+ flux measurements. All four mutants, $KCC2^{S25A}$, $KCC2^{S25D}$, $KCC2^{S26A}$, and $KCC2^{S26D}$, as well as $KCC2^{WT}$ mediated increased Tl^+ flux compared with mock-transfected cells (Fig. 4 and Table 3). Furthermore, 2 mM furosemide blocked most of the flux, demonstrating that the transport activity was largely mediated by KCC2 (Fig. 4 and Table 3) (2).

No difference in activity was detected between $KCC2^{WT}$ and KCC2 mutants or between alanine and aspartate substitutions. Previously, analysis of three N-terminal phosphorylated threonines in NKCC2 had revealed that only compound mutants resulted in altered behavior of the transporter (55). We therefore also generated the double mutants $KCC2^{S25A/S26A}$ and $KCC2^{S25D/S26D}$. Both mutants are well expressed in HEK-293 cells (Figs. 2 and 3) and showed flux activities similar to $KCC2^{WT}$ (Fig. 4 and Table 3). To ensure that our system detect differences in flux, we also determined the flux of $KCC2^{T906A}$ and $KCC2^{T1007A}$. These mutants were shown to facilitate

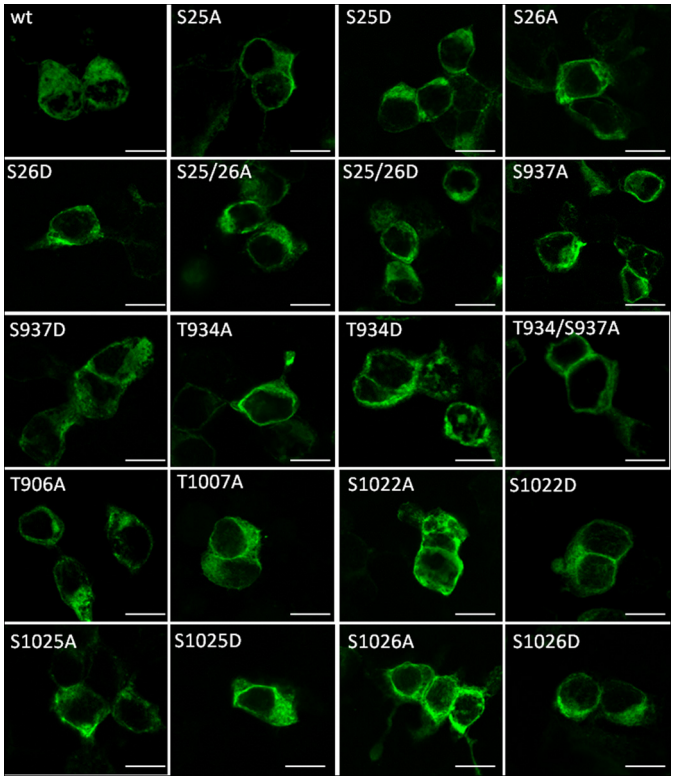

FIGURE 3. **Expression of KCC2 phospho-mutants in HEK-293 cells.** $KCC2^{WT}$ and the indicated KCC2 mutants were expressed in HEK-293 cells and efficiently delivered to the plasma membrane. The nucleus was devoid of staining. Upon visual inspection, the subcellular distribution of KCC2 mutants was indistinguishable from $KCC2^{WT}$. Photomicrographs were taken with a confocal laser scanning microscope. *Scale bar,* 10 μm.

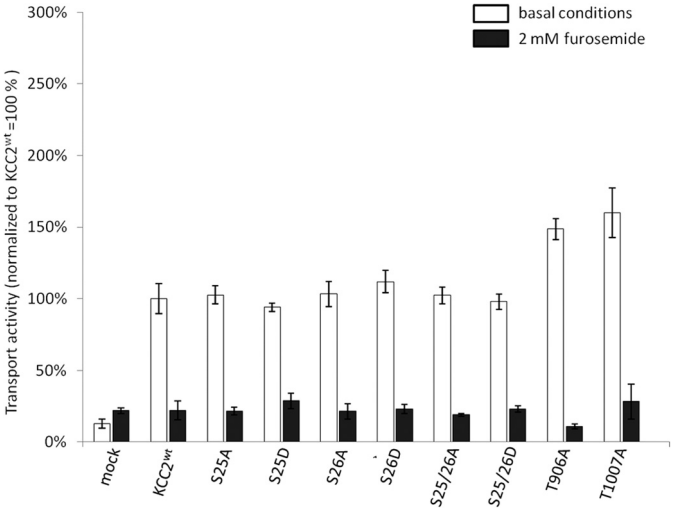

FIGURE 4. **Transport activity of N-terminal KCC2 mutants.** HEK-293 cells were transfected with $KCC2^{WT}$ and KCC2 mutant constructs, and transport activity was determined by performing Tl^+ flux measurements. Compared with $KCC2^{WT}$, the N-terminal single mutants $KCC2^{S25A}$, $KCC2^{S25D}$, $KCC2^{S26A}$, and $KCC2^{S26D}$ and the double mutants $KCC2^{S25A/S26A}$ and $KCC2^{S25D/S26D}$ showed no significant differences in transport activity. Confirming previous studies, $KCC2^{T906A}$ and $KCC2^{T1007A}$ displayed a significantly higher transport activity compared with $KCC2^{WT}$. In the presence of furosemide, the Tl^+ flux was blocked. *Graphs* represent mean ± S.E. of at least three independent measurements, normalized to $KCC2^{WT}$. Statistical analysis is presented in Table 3.

KCC2 activity (38). In keeping with the previous report, both mutants displayed a significantly increased transport activity, compared with $KCC2^{WT}$ (Fig. 4 and Table 3). These results

TABLE 3

Transport activity under basal conditions and in the presence of furosemide

	Basal conditions (significance in comparison with $KCC2^{WT}$)	2 mM furosemide (significance in comparison with untreated samples)
HEK-293	13 ± 3.2%[a]	21.9 ± 1.8% (NS)[b]
$KCC2^{WT}$	100 ± 10. 6%	22.3 ± 6.5%[a]
S25A	102.8 ± 6.6% (NS)	21.6 ± 2.6%[a]
S25D	94.1 ± 3% (NS)	28.8 ± 5.4%[a]
S26A	103.4 ± 8.9% (NS)	21.4 ± 5.5%[a]
S26D	112 ± 7.8% (NS)	23.1 ± 3%[a]
S25A/S26A	102.28 ± 5.6% (NS)	19 ± 1.1%[c]
S25D/S26D	97.9 ± 5.4% (NS)	23.1 ± 2%[c]
T906A	148.7 ± 7.3%[a]	10.9 ± 1.6%[d]
T934A	97.3 ± 2.1% (NS)	20.5 ± 3.8%[d]
T934D	226.6 ± 13%[d]	29.6 ± 8.6%[d]
S937A	106.2 ± 10.2% (NS)	21.6 ± 4.1%[d]
S937D	186.9 ± 12%[d]	16.1 ± 1.4%[d]
T934A/S937A	119.4 ± 9.8% (NS)	15.2 ± 2.9%[d]
T1007A	159.9 ± 17.4%[c]	28.3 ± 12.1%[a]
S1022A	91.3 ± 11.3% (NS)	22.5 ± 2.7%[c]
S1022D	110.8 ± 18.1% (NS)	20.7 ± 5.8%[c]
S1025A	102.2 ± 1.6% (NS)	21 ± 1.9%[d]
S1025D	99.6 ± 6.9% (NS)	18 ± 0.37%[a]
S1026A	124.2 ± 7.8% (NS)	14 ± 0.9%[d]
S1026D	115 ± 8.7% (NS)	15.4 ± 3.1%[d]

[a] $p < 0.01$.
[b] NS means not significant.
[c] $p < 0.05$.
[d] $p < 0.001$.

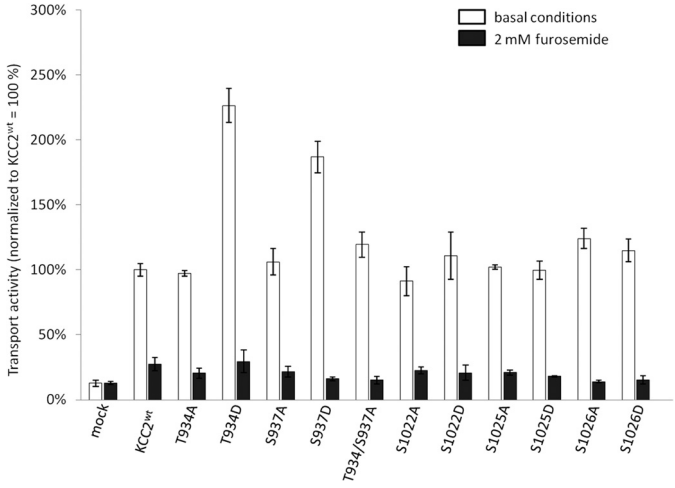

FIGURE 5. **Transport activity of C-terminal KCC2 mutants.** HEK-293 cells were transfected with $KCC2^{WT}$ and KCC2 mutant constructs, and transport activity was determined by performing Tl^+ flux measurements. The Tl^+ flux mediated by $KCC2^{S1022A}$, $KCC2^{S1022D}$, $KCC2^{S1025A}$, $KCC2^{S1025D}$, $KCC2^{S1026A}$, and $KCC2^{S1026D}$ was similar to the flux of $KCC2^{WT}$. In contrast, the phosphomimetic mutants $KCC2^{T934D}$ and $KCC2^{S937D}$ showed a significantly increased transport activity. The mutants $KCC2^{T934A}$, $KCC2^{S937A}$, and $KCC2^{T934A/S937A}$, which mimicked the dephosphorylated state, exhibited transport levels comparable with $KCC2^{WT}$. In the presence of furosemide, Tl^+ flux was blocked. *Graphs* represent the mean ± S.E. of at least three independent measurements, normalized to $KCC2^{WT}$. Statistical analysis is presented in Table 3.

revealed that our system was well suited to detect altered KCC2 transport activity. The flux data therefore demonstrate that Ser^{25} and Ser^{26} single or combined substitutions do not influence KCC2 transport activity in HEK-293 cells.

We next focused on the C-terminal phosphorylation sites. Substitution of Ser^{1022}, Ser^{1025}, and Ser^{1026} by alanine or aspartate resulted in no change in transport activity compared with KCC^{WT} (Fig. 5 and Table 3). In contrast, $KCC2^{S937D}$ mediated a furosemide-sensitive Tl^+ flux, which was significantly increased compared with $KCC2^{WT}$ (Fig. 5 and Table 3). The

phosphorylation-blocking mutant KCC2^{S937A} showed transport activity similar to KCC2^{WT} (Fig. 5 and Table 3). This result indicates that Ser^{937} is not phosphorylated in KCC2^{WT} when expressed in HEK-293 cells.

We noticed that the phosphopeptide harboring Ser^{937} also contains Thr^{934} in close proximity. In some mass spectrometric analyses of the corresponding phosphopeptide, the precise location of the phosphate group could not be determined, leading to an ambiguous status of Thr^{934} as a phosphorylation site (Table 2) (56, 57). BecauseThr^{934} and Ser^{937} demonstrated exactly the same degree of evolutionary conservation (Fig. 1), we mutated Thr^{934} as well and determined the transport activity of KCC2^{T934A} and KCC2^{T934D}. Intriguingly, KCC2^{T934D}-mediated flux was significantly facilitated compared with KCC2^{WT}, whereas KCC2^{T934A} transport activity was similar to the control (Fig. 5 and Table 3). Thus, both Thr^{934} mutants closely matched the results observed for the corresponding Ser^{937} mutants (Fig. 5). This suggests that Thr^{934} also represents a regulatory phosphorylation site. To exclude that transport activity of the single alanine mutants KCC2^{T934A} or KCC2^{S937A} was due to residual phosphorylation of the nonmutated Ser^{937} or Thr^{934}, respectively, we also generated the double mutant KCC2^{T934A,S937A}. The transport activity of this mutant was indistinguishable from that of the single mutants and of KCC2^{WT} (Fig. 5 and Table 3). These data support the notion that both amino acids are not phosphorylated in HEK-293 cells and that their phosphorylation does not contribute to the basal activity of KCC2 in this cell system. We conclude that phosphorylation of Thr^{934} or Ser^{937} represents the effective mechanisms to regulate KCC2 activity.

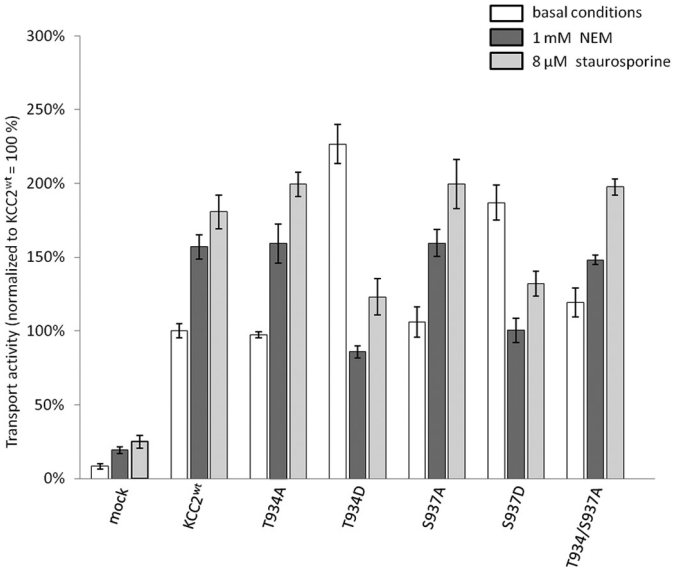

FIGURE 6. **Effect of NEM and staurosporine on the transport activity of Thr^{934} and Ser^{937} mutants.** HEK-293 cells were transfected with KCC2^{WT} and KCC2 mutant constructs and transport activity was determined by performing Tl^+ flux measurements. NEM and staurosporine were added 15 min prior to measurement. KCC2^{WT}, the single mutants KCC2^{T934A} and KCC2^{S937A}, and the double mutant KCC2$^{T934A/S937A}$ were significantly activated by NEM and staurosporine. In contrast, the activity of the mutants KCC2^{T934D} and KCC2^{S937D} was significantly reduced in the presence of NEM and staurosporine. *Graphs* represent mean ± S.E. of at least three independent measurements. Statistical analysis is presented in Table 4.

NEM and Staurosporine Effects Reverse upon Phosphorylation of Thr^{934} or Ser^{937}—NEM is one of the earliest described activators of KCC transport (2, 58). Its mode of action is still unknown, but presumably it occurs via changes in C-terminal phosphorylation (58, 59). To investigate whether Thr^{934} or Ser^{937} are involved in the NEM effect, we determined the transport activity of KCC2^{T934A}, KCC2^{T934D}, KCC2^{S937A}, KCC2^{S937D}, and KCC2^{T934A,S937A} in the presence of 1 mM NEM. In agreement with previous studies, this concentration of NEM significantly increased KCC2^{WT} transport activity (Fig. 6 and Table 4). Similarly, all three phosphorylation-blocking alanine mutants KCC2^{T934A}, KCC2^{S937A}, and KCC2^{T934A,S937A} were significantly stimulated by NEM (Fig. 6 and Table 4). This demonstrates that NEM is not acting via phosphorylation of Thr^{934} or Ser^{937}. Unexpectedly, the two phospho-mimetic mutants KCC2^{T934D} and KCC2^{S937D} were significantly inhibited by NEM and showed transport activities similar to KCC2^{WT} (Fig. 6 and Table 4). This suggests that the NEM effect is dependent on the conformational state of KCC2.

To test whether this observation is true for other stimuli as well, we applied staurosporine. This alkaloid acts as a kinase inhibitor that activates KCCs (33, 60). Staurosporine closely mimicked the effect of NEM. KCC2^{WT} as well as all three alanine mutants, KCC2^{T934A}, KCC2^{S937A}, and KCC2^{T934A,T937A}, were significantly stimulated by this kinase inhibitor, whereas the transport activity of KCC2^{T934D} and KCC2^{S937D} was significantly reduced to the level of KCC2^{WT} (Fig. 6 and Table 4). From these results, we conclude that the effect of both agents is strongly dependent on the conformational state of KCC2. Furthermore, staurosporine does not act via Thr^{934} or Ser^{937}, because the transport activities of both the alanine and the

TABLE 4
Transport activity of mutant KCC2$^{Thr-934}$ and KCC2$^{Ser-937}$ in the presence of NEM or staurosporine

	Basal conditions (significance in comparison with KCC2^{WT})	1 mM NEM (significance in comparison with untreated samples or KCC2^{WT} under basal conditions)	8 µM staurosporine (significance in comparison to the untreated samples) (or KCC2^{WT} under basal conditions)
HEK-293	8.3 ± 1.9%[a]	19.2 ± 2.2%[b]	24.8 ± 4.4%[b]
KCC2^{WT}	100 ± 4.9%	157 ± 8.2%[b]	180.7 ± 11.5%[b]
T934A	97.3 ± 2.1% (NS)[c]	159.3 ± 13%[b]	199.5 ± 8.3%[d]
T934D	226.6 ± 13%[a]	86 ± 4.1%[a] (NS)	123 ± 12.6%[a] (NS)
S937A	106.2 ± 10.2% (NS)	159.6 ± 9.3%[d]	199.5% ± 16.7%[b]
S937D	186.9 ± 12%[a]	100 ± 8.2%[a] (NS)	132.1 ± 8.5%[d] (NS)
T934A/S937A	119.4 ± 9.8% (NS)	148.2 ± 3.2%[b]	198% ± 5.4%[a]

[a] $p < 0.001$.
[b] $p < 0.05$.
[c] NS, not significant.
[d] $p < 0.01$.

aspartate mutants could still be modified by this kinase inhibitor. Finally, the concordant effects of NEM and staurosporine on the mutants suggest that both agents act via a similar mechanism. This is in agreement with the previous observation that both agents were unable to stimulate KCCs in ATP-depleted cells (61) and that deficiency of Src family kinases Fgr and Hck obliterates NEM stimulation of KCCs in red blood cells (62). Thus, NEM likely modifies KCC phosphorylation pattern in a way similar to staurosporine.

No Change in Abundance and Cell Surface Expression of $KCC2^{T934D}$ and $KCC2^{S937D}$ Mutants—Finally, we addressed the underlying mechanism of increased transport activity of $KCC2^{T934D}$ and $KCC2^{S937D}$. Altered phosphorylation might affect abundance, cell surface expression, or the transport kinetics of KCC2. To address the abundance of the KCC2 mutants, immunoblot analyses were performed for $KCC2^{T934A}$, $KCC2^{T934D}$, $KCC2^{S937A}$, and $KCC2^{S937D}$. Quantitative analysis of the immunoblots revealed no significant change in protein level (Fig. 7).

To investigate cell surface expression of the mutants, we used a previously reported KCC2 expression construct with an extracellular HA tag in the second extracellular loop between transmembrane domains 3 and 4 (48). We substituted Thr^{934} or Ser^{937} by aspartate resulting in the two new constructs $KCC2^{T934D\text{-}HA\ 2nd\ loop}$ and $KCC2^{S937D\text{-}HA\ 2nd\ loop}$. Transfection of either of the two constructs into HEK-293 cells resulted in an increased KCC2 activity, compared with $KCC2^{WT\text{-}HA\ 2nd\ loop}$, demonstrating that the HA tag did not interfere with mutations in Thr^{934} or Ser^{937} (data not shown). Surface expression of the KCC2 variants was determined in HEK-293 cells by a sandwich protocol. As a control, we used the construct $KCC2^{WT\text{-}HA\ N\text{-}term}$ with the HA tag at the intracellularly located N terminus. Surface-expressed KCC2 was labeled by incubating unfixed cells prior to permeabilization with antibodies against the extracellular HA tag for 25 min. Subsequently, cells were fixed and permeabilized, and total KCC2 was monitored using a KCC2 antibody. HEK-293 cells transfected with $KCC2^{WT\text{-}HA\ N\text{-}term}$ showed only poor labeling with anti-HA, whereas anti-cKCC2 antibodies demonstrated expression of the protein (Fig. 8*A*). In cells transfected with the HA tag in the second extracellular loop, incubation with the anti-HA antibody resulted in cell surface staining for all three constructs, $KCC2^{WT}$, $KCC2^{T934D\text{-}HA}$, and $KCC2^{S937D\text{-}HA}$ (Fig. 8*A*). Quantitative analyses of the signal ratio of surface staining to total expression revealed no difference between wild-type and mutant constructs (Fig. 8*B*), whereas significant differences in surface staining were obtained between $KCC2^{WT\text{-}HA\ N\text{-}term}$ and $KCC2^{WT\text{-}HA\ 2nd\ loop}$ ($p = 0.018$), $KCC2^{T934D\text{-}HA\ 2nd\ loop}$ ($p = 0.011$), and $KCC2^{S937D\text{-}HA\ 2nd\ loop}$ ($p = 0.027$). From this observation, we conclude that the mutations do not affect surface expression but affect the intrinsic transport activity of KCC2.

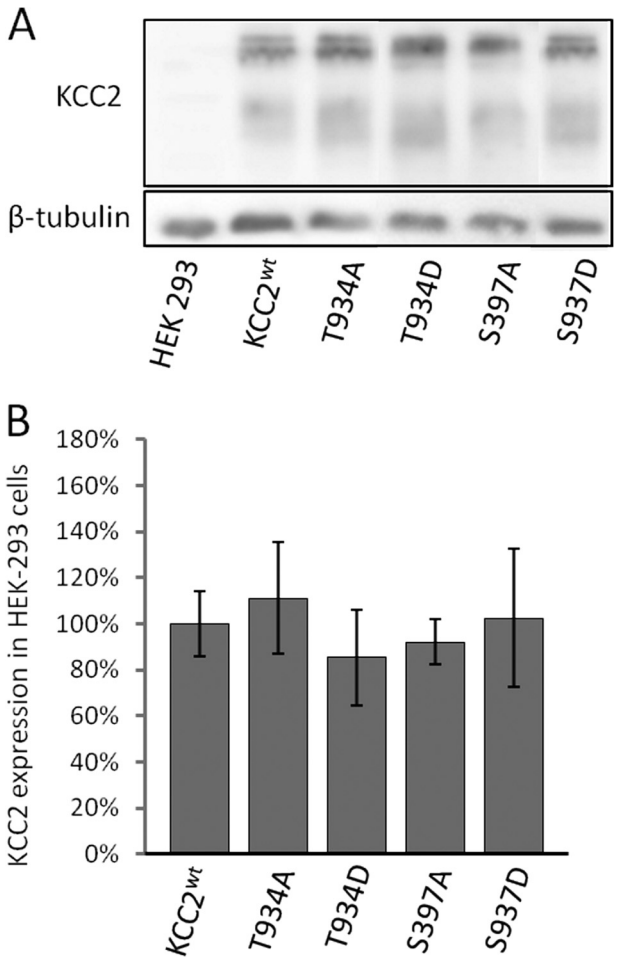

FIGURE 7. **Immunoblot analysis of $KCC2^{WT}$, $KCC2^{T934A/T934D}$, and $KCC2^{S937A/S937D}$.** *A*, KCC2 constructs were transfected into HEK-293 cells, and proteins were isolated 36 h later. 10 μg of protein were loaded onto a 10% SDS-polyacrylamide gel system, and the amount of KCC2 was determined by immunoblotting using an anti-cKCC2 antibody. KCC2-IR was detected for $KCC2^{WT}$ and KCC2 mutants, but not for mock-transfected cells, whereas β-tubulin, serving as a loading control, was present in all lanes. The figure shows one experiment out of three biological replicates with similar results. *B*, KCC2 bands were quantified and normalized to the expression of β-tubulin. This revealed no differences in the expression level between $KCC2^{WT}$ and KCC2 mutants in HEK-293 cells. *Graphs* represent mean ± S.E. of three independent experiments.

DISCUSSION

Here, we report the identification of novel potent KCC2 phosphorylation sites encompassing Ser^{937} and Thr^{934}, which are involved in kinetic regulation of the transport activity. Phospho-mimetic substitution of these two amino acid residues inverted the action of staurosporine and NEM. These results hint to a cross-talk between different phosphorylation sites and reveal the impact of the state of the transporter on the action of post-translational modifications.

Modern mass spectrometry-based *in vivo* phospho-proteomics studies have identified thousands of *bona fide* phosphorylation sites of brain proteins (56, 57, 63). So far, these publicly available data have been poorly exploited. Here, we started to investigate the possible role of such experimentally verified phosphorylation sites for regulation of KCC2 transport activity. Mutational analyses in combination with flux measurements identified a hitherto unknown potent regulatory role of Thr^{934} and Ser^{937} (Fig. 5). Substitution of these amino acids by the phospho-mimetic amino acid aspartate significantly facilitated KCC2 transport in HEK-293 cells. Thus, phosphorylation of these amino acids will enhance KCC2 transport activ-

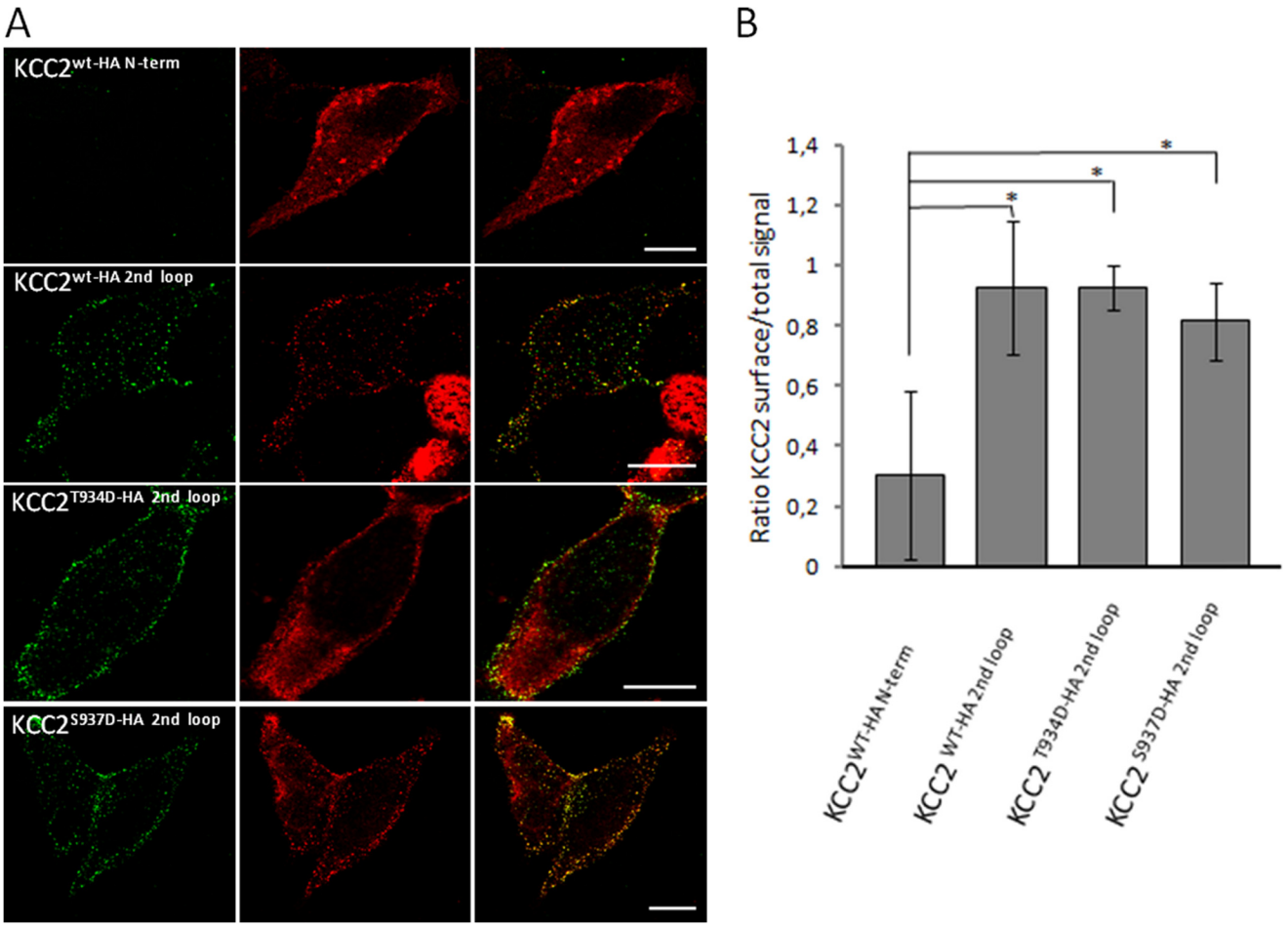

FIGURE 8. **Surface expression of KCC2 mutants in HEK-293 cells.** HEK-293 cells were transfected with the indicated constructs. Surface KCC2 (*green*) was detected using an HA antibody under nonpermeabilizing conditions and prior to fixation. After fixation and permeabilization, total KCC2 (*red*) was detected with anti-cKCC2 antibody. *A*, images show representative examples for each construct. *Scale bar*, 10 μm. *B*, ratio of surface signals to total expression signals of KCC2 was measured for each construct. Ratio of $KCC2^{WT\text{-}HA\ 2nd\ loop}$ was compared with $KCC2^{WT\text{-}HA\ N\text{-}term}$ and mutant $KCC2^{HA\ 2nd\ loop}$. Mutant $KCC2^{HA\ 2nd\ loop}$ showed no significant difference in the ratio compared with $KCC2^{WT\text{-}HA\ 2nd\ loop}$. In contrast, the ratio for the negative control $KCC2^{WT\text{-}HA\ N\text{-}term}$ was significantly reduced compared with all three other constructs. *Graphs* represent mean ± S.D. of at least three independent measurements.

ity. This is in line with the observation of phosphorylated Ser^{937} and likely Thr^{934} in adult brain tissue (57).

So far, phosphorylation mainly affected trafficking or the half-lives of KCC2 (5, 36). In contrast to these findings, the increased activity of $KCC2^{T934D}$ or $KCC2^{S937D}$ was not paralleled by an increase in total amount or cell surface expression of the transporter (Figs. 6 and 7). These results reveal a kinetic up-regulation of the transport activity by phosphorylation of these two amino acid residues. Kinetic regulation of the intrinsic transport activity of KCC2 is also suggested for Thr^{906} and Thr^{1007}, based on studies of the homologous amino acid residues Thr^{991} and Thr^{1048} in KCC3 (37). Surface biotinylation experiments demonstrated that dephosphorylation of these two threonines activated KCC3 without an increase in plasma membrane localization (37). Taken together, these data suggest a model, in which the intrinsic transport activity of KCC2 is increased by phosphorylation of Thr^{934} or Ser^{937} (this study) and decreased by phosphorylation of Thr^{906} and Thr^{1007} (37).

The prevailing notion holds that phosphorylation activates NKCCs and inactivates KCCs (31, 58, 65, 66). This elegant concept of reciprocal regulation of Cl^--inward and Cl^--outward transporters was originally based on the observations that cell swelling, NEM, staurosporine, and serine-threonine phosphatase 1 inhibited NKCC1 (67–69) and activated KCCs (33, 58, 67). This view was subsequently substantiated by the reciprocal effect of WNKs on KCCs and NKCC/NCC transport activities (31, 70) and by the fact that dephosphorylation of Thr^{906} and Thr^{1007} facilitates KCC transport (37) and phosphorylation of Tyr^{903} and Tyr^{1087} increases KCC2 degradation in lysosomes (41). However, the recent characterization of the Ser^{940} phosphorylation site of KCC2 already challenged this concept. Dephosphorylation of Ser^{940} decreased cell surface expression of KCC2 (39) and concomitantly caused depolarizing action of GABA in neurons (71). Our observation of up-regulated activity in $KCC2^{T934D}$ and $KCC2^{S937D}$ supports the emerging concept that KCC2 can both be activated and deactivated by phosphorylation, depending on the amino acid residues involved. However, the staurosporine and NEM experiments indicate that the targeted amino acid residue is not the sole determinant for the effect of phosphorylation/dephosphorylation. Both agents can have opposite effects, depending on the phosphorylation state of Thr^{934} and Ser^{937} (Fig. 6). In the dephosphorylated state, mimicked by alanine substitutions, KCC2 transport was facilitated by these two agents, and in the phosphorylated

state, represented by the aspartate mutants, the effect was the opposite. These results indicate that the conformational state of KCC2 has an impact on the functional consequences of phosphorylation/dephosphorylation of a given amino acid residue. This is reminiscent of red blood cells, where low concentrations of NEM at 0 °C activated and high concentration of NEM at 37 °C inhibited KCC-mediated transport (72).

Because of the rapid effects within minutes, NEM or staurosporine are assumed to regulate the intrinsic activity of KCCs, similar to phosphorylation of Thr^{934} or Ser^{937} (33, 58, 59). A likely explanation for the opposite effect of both agents on Thr^{934} and Ser^{937} mutants is because they induce conformational changes that differ depending on the conformational state of KCC2. In $KCC2^{WT}$, $KCC2^{T934A}$, and $KCC2^{S937A}$, they cause a state with high transport activity, whereas in $KCC2^{T934D}$ and $KCC2^{S937D}$, which have already adopted the state of high transport activity, further conformational changes imposed by indirect action of NEM or staurosporine convert KCC2 into a state of basal activity. An alternative explanation is that the conformation of $KCC2^{T934D}$ and $KCC2^{S937D}$ deoccludes a hidden site, upon which NEM or staurosporine indirectly act in a manner different from their action in $KCC2^{WT}$ (58). In either case, the data reveal a functional cross-talk between phosphorylation of Thr^{934} and Ser^{937} and another staurosporine/NEM-modulated phosphorylation site. Thus, the effect of phosphorylation can itself be modulated by phosphorylation of other sites. This might be important for fine-tuning the operational mode of KCC2 and to integrate different signaling pathways. These findings also imply that drugs aimed to modify KCC2 phosphorylation for therapeutic benefit (36, 73) have to be investigated under different conditions as their effect might depend on the conformational state of KCC2 and therefore be highly context-specific. Functional cross-talk between different regions has also been suggested for NKCC1, where phosphorylation of the N terminus causes movement of the C terminus, which in turn entails altered interactions between different transmembrane domains (74).

Among the phosphorylated amino acid residues in KCC2, Thr^{934} and Ser^{937} showed an intermediate level of evolutionary conservation. The two residues are only present in the KCC2 subgroup of vertebrate KCCs and in non-therian vertebrate KCC4 family members (Fig. 1). This is in stark contrast to Thr^{906} and Thr^{1007}, which are strongly conserved throughout evolution. Phosphorylation of Ser^{26}, which is present in most vertebrate KCC1, KCC2 and KCC4 family members, had no influence on KCC2 activity. Taken together, these data establish evolutionary conservation as a poor predictor for regulatory phosphorylation sites in KCCs. This might be expected, because subgroup-specific phosphorylation sites enable differential regulation of the diverse KCCs within the same cell. This is likely an important step favoring subfunctionalization of the different family members during vertebrate evolution (10), as they can be co-expressed in brain areas (75).

Our analyses failed to detect a regulatory role of Ser^{25}, Ser^{26}, Ser^{1022}, Ser^{1025}, and Ser^{1026} in HEK-293 cells. Ser^{25} and Ser^{26} are located in the cytoplasmic N terminus of KCC2. Previous investigations have revealed an important role of this sequence for CCC transport activity. Phosphorylation of Ser^{96} in KCC3 is involved in cell swelling-related activation of the transporter (76). Furthermore, N-terminal truncation disrupted transport activity of KCC1 (77) and KCC2 (9). In the recently identified KCC2a isoform, a SPAK-binding site with a yet unknown functional role is located in the N terminus (53). In NKCC1 and NKCC2, three N-terminally located phosphothreonines modulate transport activity (55). Interestingly, in NKCC2, mutation of either of the three threonines to alanine had no effect; mutations of two threonines resulted in reduced activity, and mutations of all three threonines blocked hypertonic activation (55). It might therefore be that mutation of more than one phosphorylated amino acid residue in the N terminus of KCC2 is required to observe a phenotype. However, the double mutants $KCC2^{S25D/S26D}$ and $KCC2^{S25A/S26A}$ demonstrated $KCC2^{WT}$-like activity as well (Fig. 4), indicating that phosphorylation of these two serines do not influence KCC2 activity in HEK-293 cells. This does not exclude a role in other processes such as trafficking of KCC2 in neurons. The C-terminal Ser^{1022}, Ser^{1025}, and Ser^{1026} are located within the so-called ISO domain of KCC2, which confers KCC2 activity under isotonic conditions (78–80). The observation that this isotonic activity of KCC2 is not influenced by the serine-threonine phosphatase inhibitor calyculin A in *Xenopus laevis* oocytes (78) supports our conclusion that phosphorylation of Ser^{1022}, Ser^{1025}, and Ser^{1026} is not required for basal KCC2 transport activity.

CONCLUSION

At least three different regulatory states of KCC2 can exist in the plasma membrane as follows: an inactive conformation, a conformation conferring basal activity, and a conformation with high transport rate. Our data reveal that Thr^{934} and Ser^{937} participate in interconversion between these conformational states and, together with Thr^{906} and Thr^{1007}, may represent key residues for kinetic regulation of KCC2. Furthermore, the varying effect of staurosporine and NEM provide evidence for a cross-talk between different phosphorylation sites. This might have implications for drug research aimed to modify KCC2 function via changes in phosphorylation.

Acknowledgments—We acknowledge the excellent technical support by M. Reents and J. Schröder. We thank F. K. Bedford for the HA-tagged KCC2 construct, J. Brocher from Biovoxxel for help with the image analyses, and Jens Schindler for help in initial experiments.

REFERENCES

1. Payne, J. A., Stevenson, T. J., and Donaldson, L. F. (1996) Molecular characterization of a putative K-Cl cotransporter in rat brain. A neuronal-specific isoform. *J. Biol. Chem.* **271,** 16245–16252
2. Payne, J. A. (1997) Functional characterization of the neuronal-specific K-Cl cotransporter: implications for $[K^+]o$ regulation. *Am. J. Physiol.* **273,** C1516–C1525
3. Rivera, C., Voipio, J., Payne, J. A., Ruusuvuori, E., Lahtinen, H., Lamsa, K., Pirvola, U., Saarma, M., and Kaila, K. (1999) The K^+/Cl^- co-transporter KCC2 renders GABA hyperpolarizing during neuronal maturation. *Nature* **397,** 251–255
4. Blaesse, P., Airaksinen, M. S., Rivera, C., and Kaila, K. (2009) Cation-chloride cotransporters and neuronal function. *Neuron* **61,** 820–838
5. Medina, I., Friedel, P., Rivera, C., Kahle, K. T., Kourdougli, N., Uvarov, P., and Pellegrino, C. (2014) Current view on the functional regulation of the

neuronal K-Cl cotransporter KCC2. *Front. Cell. Neurosci.* **8,** 27
6. Balakrishnan, V., Becker, M., Löhrke, S., Nothwang, H. G., Güresir, E., and Friauf, E. (2003) Expression and function of chloride transporters during development of inhibitory neurotransmission in the auditory brainstem. *J. Neurosci.* **23,** 4134–4145
7. Hübner, C. A., Stein, V., Hermans-Borgmeyer, I., Meyer, T., Ballanyi, K., and Jentsch, T. J. (2001) Disruption of KCC2 reveals an essential role of K-Cl cotransport already in early synaptic inhibition. *Neuron* **30,** 515–524
8. Horn, Z., Ringstedt, T., Blaesse, P., Kaila, K., and Herlenius, E. (2010) Premature expression of KCC2 in embryonic mice perturbs neural development by an ion transport-independent mechanism. *Eur. J. Neurosci.* **31,** 2142–2155
9. Li, H., Khirug, S., Cai, C., Ludwig, A., Blaesse, P., Kolikova, J., Afzalov, R., Coleman, S. K., Lauri, S., Airaksinen, M. S., Keinänen, K., Khiroug, L., Saarma, M., Kaila, K., and Rivera, C. (2007) KCC2 interacts with the dendritic cytoskeleton to promote spine development. *Neuron* **56,** 1019–1033
10. Hartmann, A. M., Tesch, D., Nothwang, H. G., and Bininda-Emonds, O. R. (2014) Evolution of the cation chloride cotransporter family: ancient origins, gene-losses, and subfunctionalization through duplication. *Mol. Biol. Evol.* **31,** 434–447
11. Gagnon, K. B., and Delpire, E. (2013) Physiology of SLC12 transporters: lessons from inherited human genetic mutations and genetically engineered mouse knockouts. *Am. J. Physiol. Cell Physiol.* **304,** C693–C714
12. Gamba, G. (2005) Molecular physiology and pathophysiology of electroneutral cation-chloride cotransporters. *Physiol. Rev.* **85,** 423–493
13. Di Fulvio, M., and Alvarez-Leefmans, F. J. (2009) in *Physiology and Pathology of Chloride Transporters and Channels in the Nervous System: From Molecules to Diseases* (Alvarez-Leefmans, F. J., and Delpire, E., eds) pp. 169–208, Elsevier/Academic Press, Inc., London, UK
14. Coull, J. A., and Gagnon, M. (2009) The manipulation of cation-chloride co-transporters as a novel means to treat persistent pain, epilepsy and other neurological disorders. *Curr. Opin. Investig. Drugs* **10,** 56–61
15. Huberfeld, G., Wittner, L., Clemenceau, S., Baulac, M., Kaila, K., Miles, R., and Rivera, C. (2007) Perturbed chloride homeostasis and GABAergic signaling in human temporal lobe epilepsy. *J. Neurosci.* **27,** 9866–9873
16. Rivera, C., Li, H., Thomas-Crusells, J., Lahtinen, H., Viitanen, T., Nanobashvili, A., Kokaia, Z., Airaksinen, M. S., Voipio, J., Kaila, K., and Saarma, M. (2002) BDNF-induced TrkB activation down-regulates the K^+-Cl^- cotransporter KCC2 and impairs neuronal Cl^- extrusion. *J. Cell Biol.* **159,** 747–752
17. Palma, E., Amici, M., Sobrero, F., Spinelli, G., Di Angelantonio, S., Ragozzino, D., Mascia, A., Scoppetta, C., Esposito, V., Miledi, R., and Eusebi, F. (2006) Anomalous levels of Cl^- transporters in the hippocampal subiculum from temporal lobe epilepsy patients make GABA excitatory. *Proc. Natl. Acad. Sci. U.S.A.* **103,** 8465–8468
18. Coull, J. A., Boudreau, D., Bachand, K., Prescott, S. A., Nault, F., Sík, A., De Koninck, P., and De Koninck, Y. (2003) Trans-synaptic shift in anion gradient in spinal lamina I neurons as a mechanism of neuropathic pain. *Nature* **424,** 938–942
19. Janssen, S. P., Truin, M., Van Kleef, M., and Joosten, E. A. (2011) Differential GABAergic disinhibition during the development of painful peripheral neuropathy. *Neuroscience* **184,** 183–194
20. Boulenguez, P., Liabeuf, S., Bos, R., Bras, H., Jean-Xavier, C., Brocard, C., Stil, A., Darbon, P., Cattaert, D., Delpire, E., Marsala, M., and Vinay, L. (2010) Down-regulation of the potassium-chloride cotransporter KCC2 contributes to spasticity after spinal cord injury. *Nat. Med.* **16,** 302–307
21. Papp, E., Rivera, C., Kaila, K., and Freund, T. F. (2008) Relationship between neuronal vulnerability and potassium-chloride cotransporter 2 immunoreactivity in hippocampus following transient forebrain ischemia. *Neuroscience* **154,** 677–689
22. Shulga, A., Thomas-Crusells, J., Sigl, T., Blaesse, A., Mestres, P., Meyer, M., Yan, Q., Kaila, K., Saarma, M., Rivera, C., and Giehl, K. M. (2008) Posttraumatic GABA(A)-mediated $[Ca^{2+}]$i increase is essential for the induction of brain-derived neurotrophic factor-dependent survival of mature central neurons. *J. Neurosci.* **28,** 6996–7005
23. Watanabe, M., Wake, H., Moorhouse, A. J., and Nabekura, J. (2009) Clustering of neuronal K^+-Cl^- cotransporters in lipid rafts by tyrosine phosphorylation. *J. Biol. Chem.* **284,** 27980–27988
24. Hartmann, A. M., Blaesse, P., Kranz, T., Wenz, M., Schindler, J., Kaila, K., Friauf, E., and Nothwang, H. G. (2009) Opposite effect of membrane raft perturbation on transport activity of KCC2 and NKCC1. *J. Neurochem.* **111,** 321–331
25. Ikeda, K., Onimaru, H., Yamada, J., Inoue, K., Ueno, S., Onaka, T., Toyoda, H., Arata, A., Ishikawa, T. O., Taketo, M. M., Fukuda, A., and Kawakami, K. (2004) Malfunction of respiratory-related neuronal activity in Na^+, K^+-ATPase $\alpha 2$ subunit-deficient mice is attributable to abnormal Cl^- homeostasis in brainstem neurons. *J. Neurosci.* **24,** 10693–10701
26. Wenz, M., Hartmann, A. M., Friauf, E., and Nothwang, H. G. (2009) CIP1 is an activator of the K^+-Cl^- cotransporter KCC2. *Biochem. Biophys. Res. Commun.* **381,** 388–392
27. Ivakine, E. A., Acton, B. A., Mahadevan, V., Ormond, J., Tang, M., Pressey, J. C., Huang, M. Y., Ng, D., Delpire, E., Salter, M. W., Woodin, M. A., and McInnes, R. R. (2013) Neto2 is a KCC2 interacting protein required for neuronal Cl^- regulation in hippocampal neurons. *Proc. Natl. Acad. Sci. U.S.A.* **110,** 3561–3566
28. Inoue, K., Yamada, J., Ueno, S., and Fukuda, A. (2006) Brain-type creatine kinase activates neuron-specific K^+-Cl^- co-transporter KCC2. *J. Neurochem.* **96,** 598–608
29. Piechotta, K., Garbarini, N., England, R., and Delpire, E. (2003) Characterization of the interaction of the stress kinase SPAK with the Na^+-K^+-$2Cl^-$ cotransporter in the nervous system– evidence for a scaffolding role of the kinase. *J. Biol. Chem.* **278,** 52848–52856
30. Piechotta, K., Lu, J., and Delpire, E. (2002) Cation chloride cotransporters interact with the stress-related kinases Ste20-kelated proline-alanine-rich kinase (SPAK) and oxidative stress response 1 (OSR1). *J. Biol. Chem.* **277,** 50812–50819
31. Kahle, K. T., Rinehart, J., de Los Heros, P., Louvi, A., Meade, P., Vazquez, N., Hebert, S. C., Gamba, G., Gimenez, I., and Lifton, R. P. (2005) WNK3 modulates transport of Cl^- in and out of cells: implications for control of cell volume and neuronal excitability. *Proc. Natl. Acad. Sci. U.S.A.* **102,** 16783–16788
32. Kelsch, W., Hormuzdi, S., Straube, E., Lewen, A., Monyer, H., and Misgeld, U. (2001) Insulin-like growth factor 1 and a cytosolic tyrosine kinase activate chloride outward transport during maturation of hippocampal neurons. *J. Neurosci.* **21,** 8339–8347
33. Khirug, S., Huttu, K., Ludwig, A., Smirnov, S., Voipio, J., Rivera, C., Kaila, K., and Khiroug, L. (2005) Distinct properties of functional KCC2 expression in immature mouse hippocampal neurons in culture and in acute slices. *Eur. J. Neurosci.* **21,** 899–904
34. Song, L., Mercado, A., Vázquez, N., Xie, Q., Desai, R., George, A. L., Jr., Gamba, G., and Mount, D. B. (2002) Molecular, functional, and genomic characterization of human KCC2, the neuronal K-Cl cotransporter. *Mol. Brain Res.* **103,** 91–105
35. Mercado, A., Song, L., Vazquez, N., Mount, D. B., and Gamba, G. (2000) Functional comparison of the K^+-Cl^- cotransporters KCC1 and KCC4. *J. Biol. Chem.* **275,** 30326–30334
36. Kahle, K. T., Deeb, T. Z., Puskarjov, M., Silayeva, L., Liang, B., Kaila, K., and Moss, S. J. (2013) Modulation of neuronal activity by phosphorylation of the K-Cl cotransporter KCC2. *Trends Neurosci.* **36,** 726–737
37. Rinehart, J., Maksimova, Y. D., Tanis, J. E., Stone, K. L., Hodson, C. A., Zhang, J., Risinger, M., Pan, W., Wu, D., Colangelo, C. M., Forbush, B., Joiner, C. H., Gulcicek, E. E., Gallagher, P. G., and Lifton, R. P. (2009) Sites of regulated phosphorylation that control K-Cl cotransporter activity. *Cell* **138,** 525–536
38. Inoue, K., Furukawa, T., Kumada, T., Yamada, J., Wang, T., Inoue, R., and Fukuda, A. (2012) Taurine inhibits K^+-Cl^- cotransporter KCC2 to regulate embryonic Cl^- homeostasis via with-no-lysine (WNK) protein kinase signaling pathway. *J. Biol. Chem.* **287,** 20839–20850
39. Lee, H. H., Walker, J. A., Williams, J. R., Goodier, R. J., Payne, J. A., and Moss, S. J. (2007) Direct protein kinase C-dependent phosphorylation regulates the cell surface stability and activity of the potassium chloride cotransporter KCC2. *J. Biol. Chem.* **282,** 29777–29784
40. Chamma, I., Heubl, M., Chevy, Q., Renner, M., Moutkine, I., Eugène, E., Poncer, J. C., and Lévi, S. (2013) Activity-dependent regulation of the K/Cl transporter KCC2 membrane diffusion, clustering, and function in hippocampal neurons. *J. Neurosci.* **33,** 15488–15503
41. Lee, H. H., Jurd, R., and Moss, S. J. (2010) Tyrosine phosphorylation reg-

ulates the membrane trafficking of the potassium chloride co-transporter KCC2. *Mol. Cell. Neurosci.* **45,** 173–179
42. Wake, H., Watanabe, M., Moorhouse, A. J., Kanematsu, T., Horibe, S., Matsukawa, N., Asai, K., Ojika, K., Hirata, M., and Nabekura, J. (2007) Early changes in KCC2 phosphorylation in response to neuronal stress result in functional downregulation. *J. Neurosci.* **27,** 1642–1650
43. Hornbeck, P. V., Kornhauser, J. M., Tkachev, S., Zhang, B., Skrzypek, E., Murray, B., Latham, V., and Sullivan, M. (2012) PhosphoSitePlus: a comprehensive resource for investigating the structure and function of experimentally determined post-translational modifications in man and mouse. *Nucleic Acids Res.* **40,** D261–D270
44. Gnad, F., Gunawardena, J., and Mann, M. (2011) PHOSIDA 2011: the post-translational modification database. *Nucleic Acids Res.* **39,** D253–D260
45. Edgar, R. C. (2004) MUSCLE: multiple sequence alignment with high accuracy and high throughput. *Nucleic Acids Res.* **32,** 1792–1797
46. Gouy, M., Guindon, S., and Gascuel, O. (2010) SeaView version 4: A multiplatform graphical user interface for sequence alignment and phylogenetic tree building. *Mol. Biol. Evol.* **27,** 221–224
47. Hartmann, A. M., Wenz, M., Mercado, A., Störger, C., Mount, D. B., Friauf, E., and Nothwang, H. G. (2010) Differences in the large extracellular loop between the K^+-Cl^- cotransporters KCC2 and KCC4. *J. Biol. Chem.* **285,** 23994–24002
48. Zhao, B., Wong, A. Y., Murshid, A., Bowie, D., Presley, J. F., and Bedford, F. K. (2008) Identification of a novel di-leucine motif mediating K^+/Cl^- cotransporter KCC2 constitutive endocytosis. *Cell. Signal.* **20,** 1769–1779
49. Hartmann, A.-M., and Nothwang, H. G. (2011) Opposite temperature effect on transport activity of KCC2/KCC4 and N(K)CCs in HEK-293 cells. *BMC Res. Notes* **4,** 526
50. Delpire, E., Days, E., Lewis, L. M., Mi, D., Kim, K., Lindsley, C. W., and Weaver, C. D. (2009) Small-molecule screen identifies inhibitors of the neuronal K-Cl cotransporter KCC2. *Proc. Natl. Acad. Sci. U.S.A.* **106,** 5383–5388
51. Blaesse, P., Guillemin, I., Schindler, J., Schweizer, M., Delpire, E., Khiroug, L., Friauf, E., and Nothwang, H. G. (2006) Oligomerization of KCC2 correlates with development of inhibitory neurotransmission. *J. Neurosci.* **26,** 10407–10419
52. King, N., Westbrook, M. J., Young, S. L., Kuo, A., Abedin, M., Chapman, J., Fairclough, S., Hellsten, U., Isogai, Y., Letunic, I., Marr, M., Pincus, D., Putnam, N., Rokas, A., Wright, K. J., Zuzow, R., Dirks, W., Good, M., Goodstein, D., Lemons, D., Li, W., Lyons, J. B., Morris, A., Nichols, S., Richter, D. J., Salamov, A., Sequencing, J. G., Bork, P., Lim, W. A., Manning, G., Miller, W. T., McGinnis, W., Shapiro, H., Tjian, R., Grigoriev, I. V., and Rokhsar, D. (2008) The genome of the choanoflagellate *Monosiga brevicollis* and the origin of metazoans. *Nature* **451,** 783–788
53. Uvarov, P., Ludwig, A., Markkanen, M., Pruunsild, P., Kaila, K., Delpire, E., Timmusk, T., Rivera, C., and Airaksinen, M. S. (2007) A novel N-terminal isoform of the neuron-specific K-Cl cotransporter KCC2. *J. Biol. Chem.* **282,** 30570–30576
54. Döding, A., Hartmann, A. M., Beyer, T., and Nothwang, H. G. (2012) KCC2 transport activity requires the highly conserved L(675) in the C-terminal β1 strand. *Biochem. Biophys. Res. Commun.* **420,** 492–497
55. Giménez, I., and Forbush, B. (2005) Regulatory phosphorylation sites in the NH2 terminus of the renal Na-K-Cl cotransporter (NKCC2). *Am. J. Physiol. Renal Physiol.* **289,** F1341–F1345
56. Schindler, J., Ye, J., Jensen, O. N., and Nothwang, H. G. (2013) Monitoring the native phosphorylation state of plasma membrane proteins from a single mouse cerebellum. *J. Neurosci. Methods* **213,** 153–164
57. Wiśniewski, J. R., Nagaraj, N., Zougman, A., Gnad, F., and Mann, M. (2010) Brain phosphoproteome obtained by a FASP-based method reveals plasma membrane protein topology. *J. Proteome Res.* **9,** 3280–3289
58. Lauf, P. K., and Adragna, N. C. (2000) K-Cl cotransport: properties and molecular mechanism. *Cell. Physiol. Biochem.* **10,** 341–354
59. Jennings, M. L., and al-Rohil, N. (1990) Kinetics of activation and inactivation of swelling-stimulated K^+/Cl^- transport. The volume-sensitive parameter is the rate constant for inactivation. *J. Gen. Physiol* **95,** 1021–1040
60. Holtzman, E. J., Kumar, S., Faaland, C. A., Warner, F., Logue, P. J., Erickson, S. J., Ricken, G., Waldman, J., Kumar, S., and Dunham, P. B. (1998) Cloning, characterization, and gene organization of K-Cl cotransporter from pig and human kidney and *C. elegans*. *Am. J. Physiol.* **275,** F550-F564
61. Flatman, P. W., Adragna, N. C., and Lauf, P. K. (1996) Role of protein kinases in regulating sheep erythrocyte K-Cl cotransport. *Am. J. Physiol.* **271,** C255–C263
62. De Franceschi, L., Fumagalli, L., Olivieri, O., Corrocher, R., Lowell, C. A., and Berton, G. (1997) Deficiency of Src family kinases Fgr and Hck results in activation of erythrocyte K/Cl cotransport. *J. Clin. Invest.* **99,** 220–227
63. Huttlin, E. L., Jedrychowski, M. P., Elias, J. E., Goswami, T., Rad, R., Beausoleil, S. A., Villén, J., Haas, W., Sowa, M. E., and Gygi, S. P. (2010) A tissue-specific atlas of mouse protein phosphorylation and expression. *Cell* **143,** 1174–1189
64. Deleted in proof
65. Kahle, K. T., Rinehart, J., and Lifton, R. P. (2010) Phosphoregulation of the Na-K-2Cl and K-Cl cotransporters by the WNK kinases. *Biochim. Biophys. Acta* **1802,** 1150–1158
66. Gagnon, K. B., England, R., and Delpire, E. (2006) Volume sensitivity of cation-Cl^- cotransporters is modulated by the interaction of two kinases: Ste20-related proline-alanine-rich kinase and WNK4. *Am. J. Physiol. Cell Physiol* **290,** C134-C142
67. Lytle, C., and McManus, T. (2002) Coordinate modulation of Na-K-2Cl cotransport and K-Cl cotransport by cell volume and chloride. *Am. J. Physiol. Cell Physiol.* **283,** C1422–C1431
68. Darman, R. B., Flemmer, A., and Forbush, B. (2001) Modulation of ion transport by direct targeting of protein phosphatase type 1 to the Na-K-Cl cotransporter. *J. Biol. Chem.* **276,** 34359–34362
69. George, J. N., and Turner, R. J. (1989) Inactivation of the rabbit parotid Na/K/Cl cotransporter by *N*-ethylmaleimide. *J. Membr. Biol.* **112,** 51–58
70. Kahle, K. T., Rinehart, J., Ring, A., Gimenez, I., Gamba, G., Hebert, S. C., and Lifton, R. P. (2006) WNK protein kinases modulate cellular Cl^- flux by altering the phosphorylation state of the Na-K-Cl and K-Cl cotransporters. *Physiology* **21,** 326–335
71. Lee, H. H., Deeb, T. Z., Walker, J. A., Davies, P. A., and Moss, S. J. (2011) NMDA receptor activity downregulates KCC2 resulting in depolarizing GABAA receptor-mediated currents. *Nat. Neurosci.* **14,** 736–743
72. Lauf, P. K., and Adragna, N. C. (1995) Temperature-induced functional deocclusion of thiols inhibitory for sheep erythrocyte K-Cl cotransport. *Am. J. Physiol.* **269,** C1167–C1175
73. Gagnon, M., Bergeron, M. J., Lavertu, G., Castonguay, A., Tripathy, S., Bonin, R. P., Perez-Sanchez, J., Boudreau, D., Wang, B., Dumas, L., Valade, I., Bachand, K., Jacob-Wagner, M., Tardif, C., Kianicka, I., Isenring, P., Attardo, G., Coull, J. A., and De Koninck, Y. (2013) Chloride extrusion enhancers as novel therapeutics for neurological diseases. *Nat. Med.* **19,** 1524–1528
74. Monette, M. Y., Somasekharan, S., and Forbush, B. (2014) Molecular motions involved in Na-K-Cl cotransporter-mediated ion transport and transporter activation revealed by internal cross-linking between transmembrane domains 10 and 11/12. *J. Biol. Chem.* **289,** 7569–7579
75. Becker, M., Nothwang, H. G., and Friauf, E. (2003) Differential expression pattern of chloride cotransporters NCC, NKCC2, KCC1, KCC3, KCC4 and AE3 in the developing rat auditory brainstem. *Cell Tissue Res.* **312,** 155–165
76. Melo, Z., de los Heros, P., Cruz-Rangel, S., Vázquez, N., Bobadilla, N. A., Pasantes-Morales, H., Alessi, D. R., Mercado, A., and Gamba, G. (2013) N-terminal serine dephosphorylation is required for KCC3 cotransporter full activation by cell swelling. *J. Biol. Chem.* **288,** 31468–31476
77. Casula, S., Shmukler, B. E., Wilhelm, S., Stuart-Tilley, A. K., Su, W., Chernova, M. N., Brugnara, C., and Alper, S. L. (2001) A dominant negative mutant of the KCC1K-Cl cotransporter–Both N- and C-terminal cytoplasmic domains are required for K-Cl cotransport activity. *J. Biol. Chem.* **276,** 41870–41878
78. Mercado, A., Broumand, V., Zandi-Nejad, K., Enck, A. H., and Mount, D. B. (2006) A C-terminal domain in KCC2 confers constitutive K^+-Cl^- cotransport. *J. Biol. Chem.* **281,** 1016–1026
79. Acton, B. A., Mahadevan, V., Mercado, A., Uvarov, P., Ding, Y., Pressey, J., Airaksinen, M. S., Mount, D. B., and Woodin, M. A. (2012) Hyperpolarizing GABAergic transmission requires the KCC2 C-terminal ISO domain. *J. Neurosci.* **32,** 8746–8751
80. Bergeron, M. J., Gagnon, E., Caron, L., and Isenring, P. (2006) Identification of key functional domains in the C terminus of the K^+-Cl^- cotransporters. *J. Biol. Chem.* **281,** 15959–15969

Neurobiology:

A Novel Regulatory Locus of Phosphorylation in the C Terminus of the Potassium Chloride Cotransporter KCC2 That Interferes with *N*-Ethylmaleimide or Staurosporine-mediated Activation

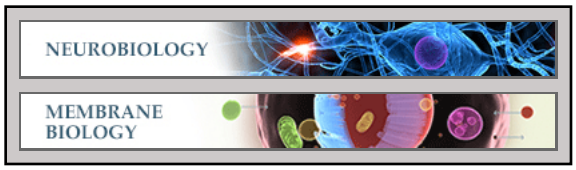

Maren Weber, Anna-Maria Hartmann, Timo Beyer, Anne Ripperger and Hans Gerd Nothwang

J. Biol. Chem. 2014, 289:18668-18679.
doi: 10.1074/jbc.M114.567834 originally published online May 21, 2014